Articles

Development of a Binding Model to Protein Tyrosine Kinases for Substituted Pyrido[2,3-*d*]pyrimidine Inhibitors[‖]

Susanne Trumpp-Kallmeyer,*,[‡] J. Ronald Rubin,[‡] Christine Humblet,[‡] James M. Hamby,[†] and H. D. Hollis Showalter[†]

Parke-Davis Pharmaceutical Research, Division of Warner-Lambert Company, 2800 Plymouth Road, Ann Arbor, Michigan 48105

Received September 19, 1997

Previously, our laboratories have reported on a new class of highly potent tyrosine kinase inhibitors based on the pyrido[2,3-*d*]pyrimidine core template. To understand the structural basis for the potency and specificity, a model for the binding mode of this class of inhibitors to the tyrosine kinase domains of c-Src, PDGFr, FGFr, and EGFr tyrosine kinases was developed from structural information (principally utilizing the catalytic domain of c-AMP-dependent protein kinase as template) and structure−activity relationship (SAR) information. In the resulting docking mode, the pyrido[2,3-*d*]pyrimidine template shows a hydrogen-bonding pattern identical to that of olomoucine. The 6-aryl substituent of the heterocycle is located deep in the binding cleft in a pocket not used by ATP, which helps to confer high-affinity binding as well as specificity. The 2-anilino and 2-(dialkylamino)alkylamino substituents as well as the 7-urea substituent of inhibitors within this class are located at the entrance of the binding cleft and make contact with residues in the hinge region between the two kinase lobes. This allows considerable variability and bulk tolerance for C-2 and N-7 substituents. The models presented here are consistent with the SAR seen for the inhibition of a number of isolated enzymes and provide a structural basis to explain their specificity. They have been used successfully to design new highly potent protein kinase inhibitors.

Introduction

Signaling for a large number of cellular functions, including cell growth and differentiation, is modulated by a variety of receptor and nonreceptor protein tyrosine kinases and their ability to phosphorylate tyrosine residues in specific proteins.[1] Abnormal signaling via tyrosine kinases has been linked to a number of pathophysiological processes including cancer, cardiovascular diseases, and immunoinflammatory diseases. Thus, for example, the growth factors from platelet-derived growth factor (PDGF), epidermal growth factor (EGF), and fibroblast growth factor (FGF) are important in the proliferative responses of vascular smooth muscle cells after balloon angioplasty.[2−4] These growth factors and their receptors are also upregulated in some types of cancer including colon, breast, ovarian, and bladder cancer.[5] As part of a therapeutic intervention against these diseases, we have been interested in the development of small molecule inhibitors of the PDGF, FGF,

Figure 1. High-throughput screening hits for receptor tyrosine kinases from structural classes A and B.

and EGF receptor tyrosine kinases and the c-Src nonreceptor tyrosine kinase.

Previous reports from our laboratories have described several series of potent tyrosine kinase inhibitors that are based on lead structures A and B identified through compound library screening (Figure 1).[6] Each lead possesses the pyrido[2,3-*d*]pyrimidine heterocycle as the core pharmacophore and displays ATP-competitive inhibition. From these a large number of potent analogues have been derived with variable substituents at the C-2, C-6, C-7, and N-8 positions.[7−9] Some of these inhibitors are highly selective for FGFr kinase, but others are broadly active against a number of tyrosine kinases. All of them are completely inactive against the cyclin-dependent kinases screened thus far.

To understand the structural basis for their potency and specificity and to rationalize the observed structure−activity relationships (SAR), we were interested in identifying the binding mode of this class of compounds to several protein tyrosine kinases.

Figure 2. ATP docked into the 3D model of chicken c-Src kinase. The adenine base of ATP forms two hydrogen bonds with the backbone carbonyl of Glu 339 and the amide hydrogen of Met 341 located on the extended coil stretch. The 2′-OH group is hydrogen bonded to Ser 345. Lys 295 forms electrostatic interactions with the α- and β-phosphate of ATP, and Arg 388 interacts with the γ-phosphate of ATP.

In this paper, we discuss the construction of molecular models for the tyrosine kinase domains of EGFr, PDGFr, FGFr, and c-Src tyrosine kinases using the X-ray structure of the ternary complex of the catalytic subunit of cAMP-dependent protein kinase A (PKA) as template.[10] Then, using the 3D models of the tyrosine kinases, the SAR data from the pyrido[2,3-d]pyrimidine inhibitor series, and structural information from other protein kinases complexed with different ATP-competitive inhibitors,[11] a possible binding mode is identified. We further discuss this binding mode in the context of the potency and selectivity of these compounds.

Structure of Protein Tyrosine Kinase Catalytic Domains

A comparison of the primary sequences of core tyrosine kinase domains reveals both conserved and divergent motifs that permit classification of a superfamily of more than 500 members into subfamilies.[12] The homology in primary sequences predicts that their 3D structures will resemble that of the catalytic subunit of PKA, which was the first protein kinase for which the 3D crystal structure became available.[10] X-ray structures of other members of the protein kinase family have recently appeared in the literature, all confirming and enhancing our knowledge of the 3D architecture of the ATP binding region.[13−18]

The catalytic site of protein kinases consists of two domains separated by a deep cleft. The smaller N-terminal domain contains the ATP binding site and consists primarily of antiparallel β-strands and one α-helix. The larger C-terminal domain is predominantly helical in structure and functions in peptide binding and catalysis. The cleft between the two lobes provides a pocket in which ATP and a portion of the substrate are positioned for phosphate transfer. The ATP binding site is a common structural theme of the entire protein kinase family and is defined by two β-sheets that form a narrow binding cleft for ATP between the N- and C-terminal lobes. A conserved ATP binding mode has

Table 1. SAR Survey for Structural Class A
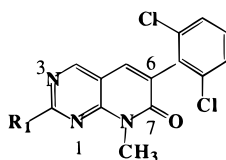
compd	R$_1$	IC$_{50}$ (μM)			
		PDGFr	FGFr	c-Src	EGFr
1	NH$_2$	4.87	1.32	0.26	5.6
2	H	>50	>50	>10	>50
3	Me	>50	>50	>50	>50
4	NMe$_2$	>50	>50	>50	>50
5	NHPh	0.33	0.51	0.024	0.078
6	NH(CH$_2$)$_3$-N-Me-piperazine	2.70	0.348	0.237	8.7
7	NH(CH$_2$)$_3$-morpholine	6.3	1.26	0.53	nd
8	NH(CH$_2$)$_3$NEt$_2$	8.85	1.97	0.96	1.35
9	NHPh(4-OCH$_2$CH$_2$NEt$_2$)	0.096	0.044	0.009	0.35
10	NHPh(3-OCH$_2$CH$_2$NEt$_2$)	0.103	0.048	0.009	nd
11	NHPh(4-CH$_2$CO$_2$H)	0.070	0.061	0.010	nd
12	NHPh(4-piperazine-NMe)	0.115	0.051	0.010	nd

been observed in several recently published protein kinase structures, which is in agreement with the high degree of sequence and structure identity present in the catalytic core of protein kinases.

For example in the 3D model of c-Src kinase, the adenine base is anchored by a bidentate hydrogen bond donor−acceptor system (Figure 2); the hydrogen bond between N-6 hydrogen of adenine and the backbone carbonyl of Glu 339 and the hydrogen bond between N-1 of adenine and the backbone amide of Met 341 fix the purine to the extended coil stretch connecting the N-terminal lobe with the C-terminal lobe of the enzyme. The third hydrogen bond, found in PKA between the N-7 hydrogen of adenine and the side-chain hydroxyl of Thr 183, located on strand 8 preceding the activation loop, is not conserved in c-Src and some other protein kinases, due to an Ala (Ala 403) exchange. This suggests that this hydrogen bond might not be essential for ATP binding. Nonpolar interactions with one side of the purine ring occur with Ala 293 on strand 3 and with Val 281 and Leu 273, which form part of the conserved glycine-rich flap. Nonpolar interactions from the opposite site result from binding of Leu 393 on strand 7 and Ala 403 on strand 8. The ribose and the triphosphate moieties extend toward the opening of the cleft where phosphate transfer occurs. The 2′-OH of the ribose ring can form a hydrogen bond with Ser 345 located on the extended coil stretch that connects the N-terminal with the C-terminal loop. The triphosphate moiety of ATP is located close to the Gly-rich loop and is fixed by a number of conserved residues in the N- and C-terminal domains as well as two magnesium ions (Figure 2).

Despite the high degree of residue conservation in the ATP binding site of protein tyrosine kinases, some amino acid differences are present (see Figure 2). The entrance of the binding pocket in c-Src, possessing the Ser 345 residue, is considerably more hydrophobic than the corresponding pocket in PDGFr (Asp 687) and FGFr (Asn 568). This region is also more spacious in c-Src, due to the presence of the amino acid sequence Arg 388, Ala 389, Ala 390. This sequence is reversed in PDGFr, FGFr, and EGFr to Ala, Ala, Arg, respectively, which slightly narrows the entrance of the ATP binding pocket.

Furthermore, there are several amino acid differences deep in the cleft, in a hydrophobic pocket adjacent to the ATP binding site (Figure 2 and alignment in Figure 7). In particular, Val 323 on strand 4 in c-Src and Val 664 in PDGFr correspond to Ile 545 in FGF and Cys 751 in EGFr. Ile 336 on strand 5 in c-Src and PDGFr (Ile 678) corresponds to Val 559 and Leu 768 in EGFr. The threonine on strand 5 in c-Src (Thr 338) and PDGFr (Thr 680) as well as EGFr (Thr 766) corresponds to Val 561 in FGFr. Finally, Ala 403 on strand 8 in c-Src and FGFr (Ala 640) corresponds to Thr 830 in EGFr and Cys 842 in PDGFr. With the exception of Thr 830 in EGFr and Cys 842 in PDGFr, these amino acids are not involved in ATP binding but might be important for inhibitor binding and thus might influence inhibitor potency and selectivity.

Identification of a Possible Binding Mode for the Pyrido[2,3-*d*]pyrimidine Type Inhibitors

The SAR derived for the pyrido[2,3-*d*]pyrimidines was essential in formulating a binding mode for this class of inhibitors. The basic pharmacophore of the lead compounds, A and B (Table 1), is the pyrido[2,3-*d*]-pyrimidine heterocycle. The C-2 amino moiety is absolutely essential, and replacement of it by a C-2 methyl group completely abolishes activity (see Table 1; compounds **1**−**3**). Monosubstitution of the 2-NH$_2$ group with a large number of dialkylaminoalkyl side chains (Table 1; compounds **6**−**8**) as well as aryl side chains substituted with acidic or basic functionality (Table 1; compounds **5**, **9**−**12**) improves potency as well as solubility. However, disubstitution of the 2-NH$_2$ group completely abolishes the activity, indicating that a 2-NHR function is essential, presumably to provide a hydrogen bond donor. Replacement of the N-3 with carbon within the core template also abolishes activity, suggesting an essential role of this nitrogen as a potential hydrogen bond acceptor. Within the B series, a large number of substituted ureas are tolerated in the N-7 position (Table 2). For the phenyl moiety at C-6, replacement with larger substituents markedly reduces activity (Table 3; compounds **18**, **20**). However, subtle modifications in the 3- and 5-positions of the pendant phenyl ring can exert a pronounced effect on selectivity.

Table 2. SAR Survey of Structural Class B
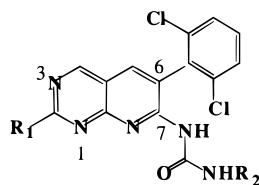
			IC$_{50}$ (μM)			
compd	R$_1$	R$_2$	PDGFr	FGFr	c-Src	EGFr
13	NH(CH$_2$)$_4$NEt$_2$	*t*-Bu	0.36	0.048	0.023	0.39
14	NH(CH$_2$)$_3$-N-Me-piperazine	cyclohexyl	0.263	0.040	0.031	0.88
15	NH(CH$_2$)$_3$-N-Me-piperazine	Ph-4-OCH$_3$	0.793	0.139	0.028	0.720
16	NH(CH$_2$)$_3$-N-Me-piperazine	benzyl	1.98	0.125	0.03	0.98
17	NHPh(4-OCH$_2$CH$_2$NEt$_2$)	*t*-Bu	1.1	0.051	0.024	nd

Table 3. SAR Survey of FGFr-Selective Compounds of Structural Classes A and B
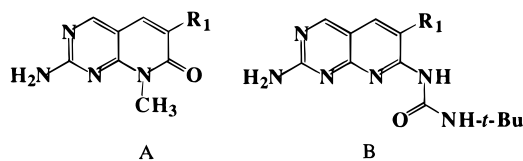
			IC$_{50}$ (μM)			
compd	formula	R$_1$	PDGFr	FGFr	c-Src	EGFr
18	B	Ph(3,5-diNMe$_2$)	>50	>16	>50	nd
19	B	Ph(3,5-diCF$_3$)	>50	>50	>50	nd
20	B	Ph(3,5-diOEt)	>50	1.65	>50	nd
21	B	Ph(3,5-diOMe)	>50	0.06	>50	50
22	A	Ph(3,5-diOMe)	43.1	0.126	>50	nd

For example, inhibitors with 3,5-dimethoxyphenyl substitution show high selectivity for FGFr kinase (Table 3; compounds **21**, **22**).

X-ray structural information obtained from protein kinases with bound ATP and competitive inhibitors was also used to identify the binding mode of the pyrido-[2,3-*d*]pyrimidine inhibitors. In particular, the ATP-competitive inhibitor olomoucine, which has been co-crystallized with CDK2, gave information on how our inhibitors might bind in the ATP binding site. The base adenine of olomoucine shows formation of two hydrogen bonds with the backbone of the extended coil stretch, which is different from the hydrogen-bonding motif of this enzyme to the adenine of ATP.[11] Although the purine ring of olomoucine binds roughly into the same area of the binding cleft as the adenine ring of ATP, the orientation of the purine ring with respect to the protein is different.

In particular, for olomoucine one hydrogen bond is formed between N-7 of the adenine base and the backbone NH of Leu 83, which normally forms a hydrogen bond to the N-1 of adenine. Glu 81 which normally forms a hydrogen bond to the 6-NH$_2$ of adenine does not form a corresponding hydrogen bond with olomoucine. Instead, a second hydrogen bond is formed with the backbone carbonyl of Leu 83, which is located closer to the entrance of the ATP binding pocket.[11] This indicates that ATP-competitive inhibitors form hydrogen bonds within the extended coil stretch of the enzyme, but depending on substitution patterns in their structure, the binding mode can change and different amino acids within this coil are involved.

A structural comparison of ATP and olomoucine with our pyrido[2,3-*d*]pyrimidine inhibitors reveals that a bidendate hydrogen bond donor−acceptor motif is also present in this class (Figure 3). As discussed above, SAR studies indicate an essential role for N-3 and the exocyclic 2-NHR within the pyrido[2,3-*d*]pyrimidine template, suggesting that they might form hydrogen bonds with the peptide backbone of the extended coil stretch, similar to that of ATP or olomoucine binding.

To construct a possible inhibitor binding mode, docking studies were performed with the pyrido[2,3-*d*]-pyrimidine nucleus of compounds **9**, **11**, and **17** (Tables 1 and 2) starting with different initial orientations of the heterocyclic ring in the ATP binding pocket of the 3D model of c-Src. Two different low-energy conformations of the aniline ring substituent, relative to the pyrido[2,3-*d*]pyrimidine heterocycle, were used for these studies. In one conformation, the aniline substituent was placed vicinal to N-1 and in the second vicinal to N-3. Both conformations correspond to local minima with energy values of 7.05 and 6.99 kcal, respectively (see Experimental Section). The amino acid side chains were reoriented to relieve unfavorable steric interactions, and the complexes were subsequently energy-minimized. The SAR data were weighted more heavily than the interaction energies in choosing the most plausible interaction complex.

We initially thought that inhibitors of the pyrido[2,3-*d*]pyrimidine class would possess a hydrogen-bonding pattern identical to that of the adenine base of ATP. However, after careful docking studies, we excluded this binding motif due to major unfavorable steric interactions of the 2-anilino substituent with β-strands 1−3 and the extended coil stretch. Instead, we have adopted the binding motif of olomoucine, which does not show bad steric interactions and satisfies all the SAR data described above. In this binding mode, the N-3 of the pyrido[2,3-*d*]pyrimidine template forms a hydrogen bond to the backbone NH of Met 341 in c-Src (or the corresponding amino acid in FGFr, EGFr, and PDGFr kinases). This hydrogen bond is analogous to the hydrogen bond between the N-7 of olomoucine and the backbone NH of Leu 83 in CDK2.[11] A second hydrogen bond can be formed between the exocyclic 2-amino hydrogen of the heterocycle and the carbonyl oxygen of Met 341. This is analogous to the hydrogen bond between N-6 hydrogen of olomoucine and the backbone carbonyl of Leu 83 in CDK2.[11] The 2-anilino substituent

ATP Olomoucine 1

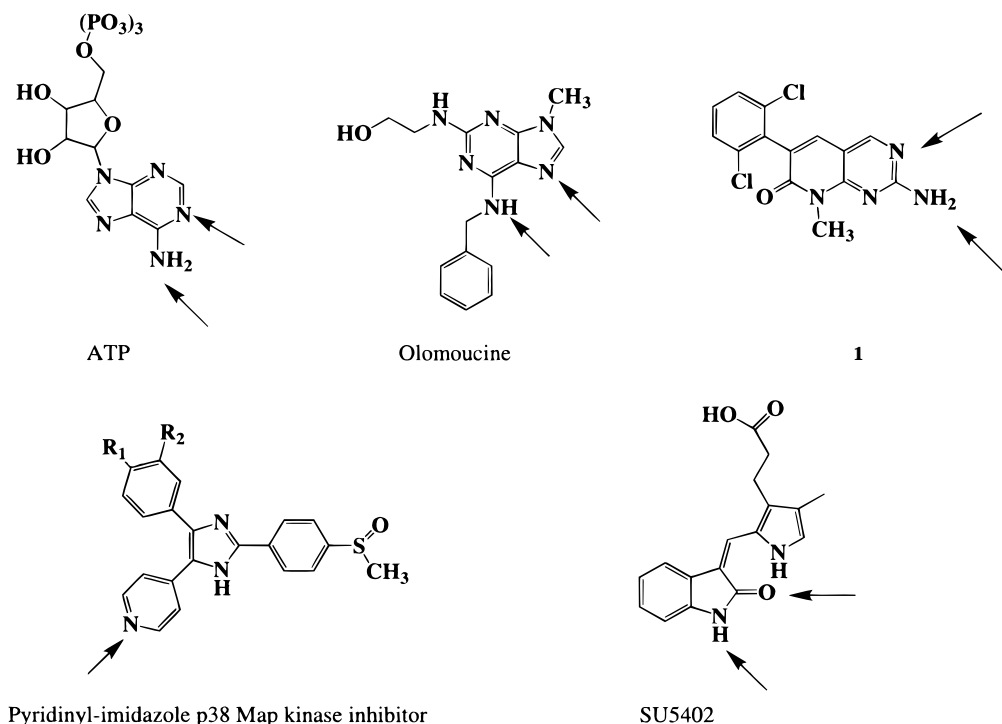Pyridinyl-imidazole p38 Map kinase inhibitor SU5402

Figure 3. ATP, olomoucine, compound **1** (Table 1), the pyridinylimidazole p38 MAP kinase inhibitor, and Su5402 with hydrogen-bonding donor and acceptor indicated with arrows.

is located vicinal to N-1 of the pyrido[2,3-*d*]pyrimidine template with the phenyl ring rotated out of plane by approximately 30° and can form favorable interactions with the extended coil stretch and β-strand 1.

For this class of inhibitors, the 6-phenyl substituent is located in a deep pocket of moderate size adjacent to the adenine binding pocket. This pocket is utilized specifically by this class, but not by ATP, and is made up of Ile 336 and Thr 338 on strand 5, Val 323 on strand 4, Ala 403, Asp 404, and Phe 405 on strand 8, and Glu 310 and Met 314 on the αC helix. The 6-phenyl substituent is located close to Thr 338 on strand 5 to which it can form an aromatic hydrogen bond. The 7-carbonyl substituent of the pyrido[2,3-*d*]pyrimidine heterocycle can form a hydrogen bond with Lys 295 on strand 3, which normally hydrogen-bonds oxygens from the α- and β-phosphate group of ATP (Figure 4). Similarly in compound class B the carbonyl of the 7-urea substituent forms a hydrogen bond with Lys 295 (Figure 5). The 2-aminoaryl or alkyl substituent is located at the entrance of the ATP binding pocket. The dialkyl-aminoalkyl substituents of compounds **6**−**8** protude out of the binding pocket and are solvent-exposed. The 2-aminophenyl substituents of compounds **9**−**12** (Table 1) and **17** (Table 2) can form additional interactions with the peptide backbone and amino acid side chains of the extended coil stretch. Figure 4 shows compound **9** docked into the ATP binding pocket of the 3D model of c-Src kinase.

For structural series B, the substituted urea appended to the C-7 position is located at the entrance of the pocket near the binding site for the ribose ring of ATP. The large cyclohexyl, benzyl, or phenyl substituents of the urea extend out of the binding pocket and reach out to residues located in the hinge region. In Figure 5 compound **17** is shown docked into the ATP binding pocket of c-Src kinase.

This inhibitor−enzyme model satisfies most of the observed SAR for this class of inhibitors. Our data (unpublished) show that when the N-3 of the pyrido-[2,3-*d*]pyrimidine heterocycle is replaced by carbon, binding affinity is completely abolished. Binding is also lost when the 2-amino function is disubstituted or replaced by methyl or hydrogen (Table 1). This confirms the importance of the presence of both nitrogens to form a bidentate hydrogen bond acceptor−donor system as formulated in the model. The model shows that the distal dialkylaminoalkyl substituents off the 2-amino group extend out of the binding pocket and are exposed to solvent. This is in agreement with the inhibitor SAR which shows that potency of the inhibitors is increased only marginally by substitution of the 2-NH$_2$ group with various flexible alkyl side chains (Tables 1 and 2). Within structural series A and B, the generally greater increase in affinity that is observed when the 2-NH$_2$ group is substituted with different aryl side chains can be attributed to additional interactions of the aniline ring with the extended coil stretch and with residues located in the hinge region (Figure 4). In series B, substitution of the urea with large alkyl or aryl side chains does not significantly affect potency, supporting the model which shows that large substituents off the distal urea nitrogen are located at the entrance of the pocket and are solvent-exposed. The 7-carbonyl function of compound class A as well as the 7-urea function of compound class B is necessary for good tyrosine kinase potency as removal or exchange of both functions decreases the binding affinity.[6] In the 3D models the 7-carbonyl as well as the carbonyl function in the 7-urea substituent can form an electrostatic hydrogen bond with Lys 295, which normally interacts with the α- and β-phosphate of ATP. (An ORTEP diagram of the X-ray structure of **13** is shown in Figure 6.)
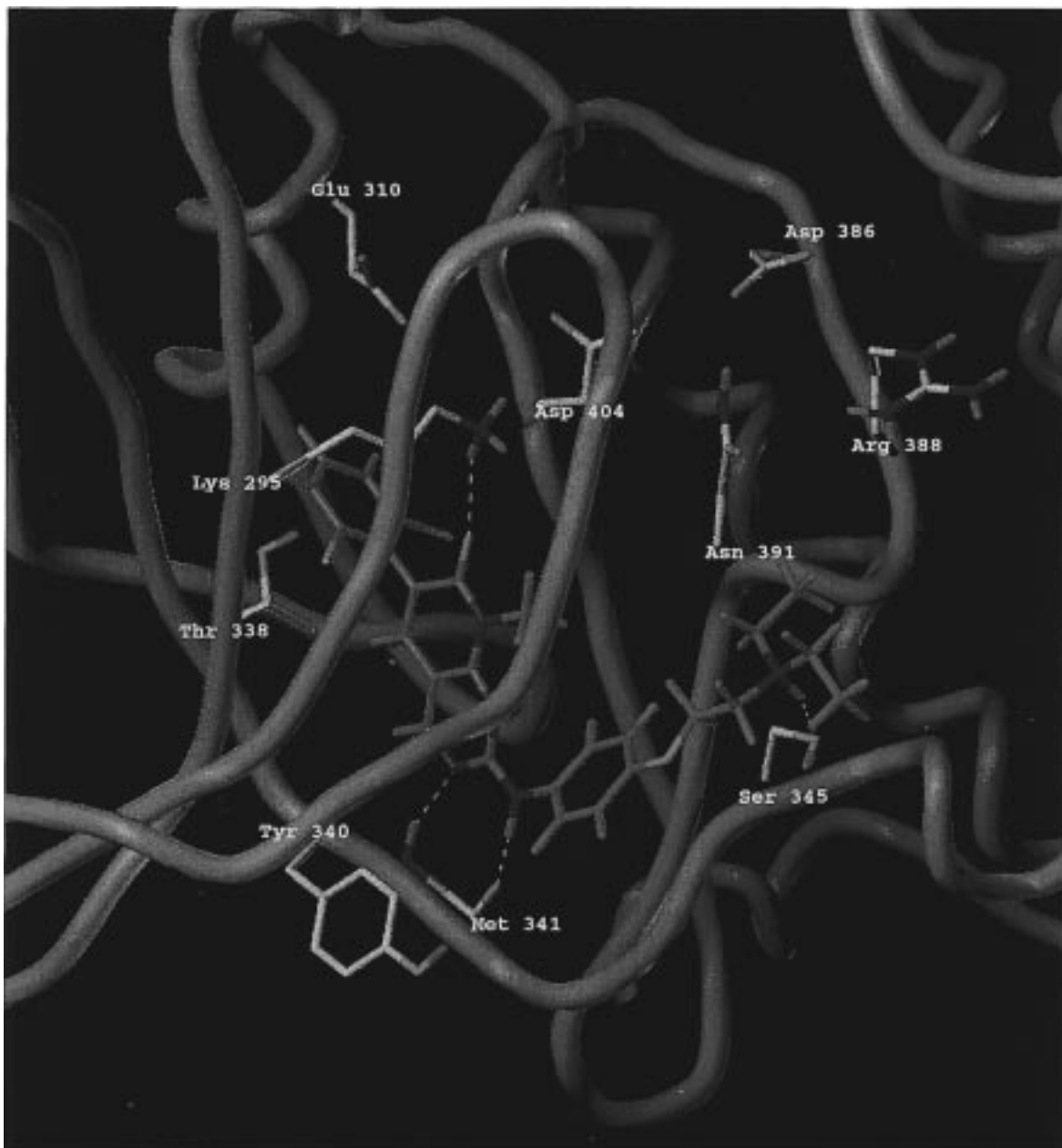
Figure 4. Compound **9** (Table 1) docked into the 3D model of the ATP binding site of c-Src. The pyrido[2,3-*d*]pyrimidine template has a hydrogen-bonding pattern identical to that observed for olomoucine in CDK2. In this binding mode, N-3 of the pyrido[2,3-*d*]pyrimidine template forms a hydrogen bond to the NH backbone of Met 341 in c-Src. A second hydrogen bond can be formed with the exocyclic 2-amino hydrogen and the carbonyl oxygen of Met 341. A third hydrogen bond might be formed with the 7-carbonyl substituent and Lys 295. The 6-dichlorophenyl substituent is located in a deep pocket consisting of strands 4, 5, and 8 and the αC helix. The 6-phenyl substituent can form an aromatic hydrogen bond with Thr 338. The 2-anilino substituent is located at the entrance of the binding pocket with the solubilizing group contacting residues in the hinge region.

The observation that replacement of chlorine with larger substituents on the C-6 phenyl moiety leads to a large reduction in binding affinity (Table 3) is in agreement with the location of this ring in a deep well-defined pocket of restricted size. Additionally, binding energy may be provided by the two chlorine substitutents off the ortho positions of the phenyl ring. Recent publications show that this same pocket is occupied by other potent protein kinase inhibitors. For the highly potent pyridinylimidazole p38 MAP kinase inhibitors, the 4-phenyl ring is located in the same binding site and confers high affinity and selectivity.[19] A single residue in this pocket (Thr 106 on strand 5) has been identified as being responsible for the selectivity.[19] The 3-bromo-

anilino ring of the highly potent and selective quinazoline EGFr inhibitors is proposed to be located in a similar location and is likely responsible for the exceptional binding affinity and selectivity of this class of compounds.[20]

Structural differences in this pocket between c-Src and other closely related tyrosine kinases may in part explain different specificity patterns observed when subtle modifications are made in the 6-phenyl substituent. For example, 3,5-dimethoxyphenyl substitution (Table 3) results in high selectivity toward the FGFr tyrosine kinase, whereas the 2,6-dichlorophenyl substituent confers inhibition toward a range of tyrosine kinases (Tables 1 and 2). As mentioned above, in this
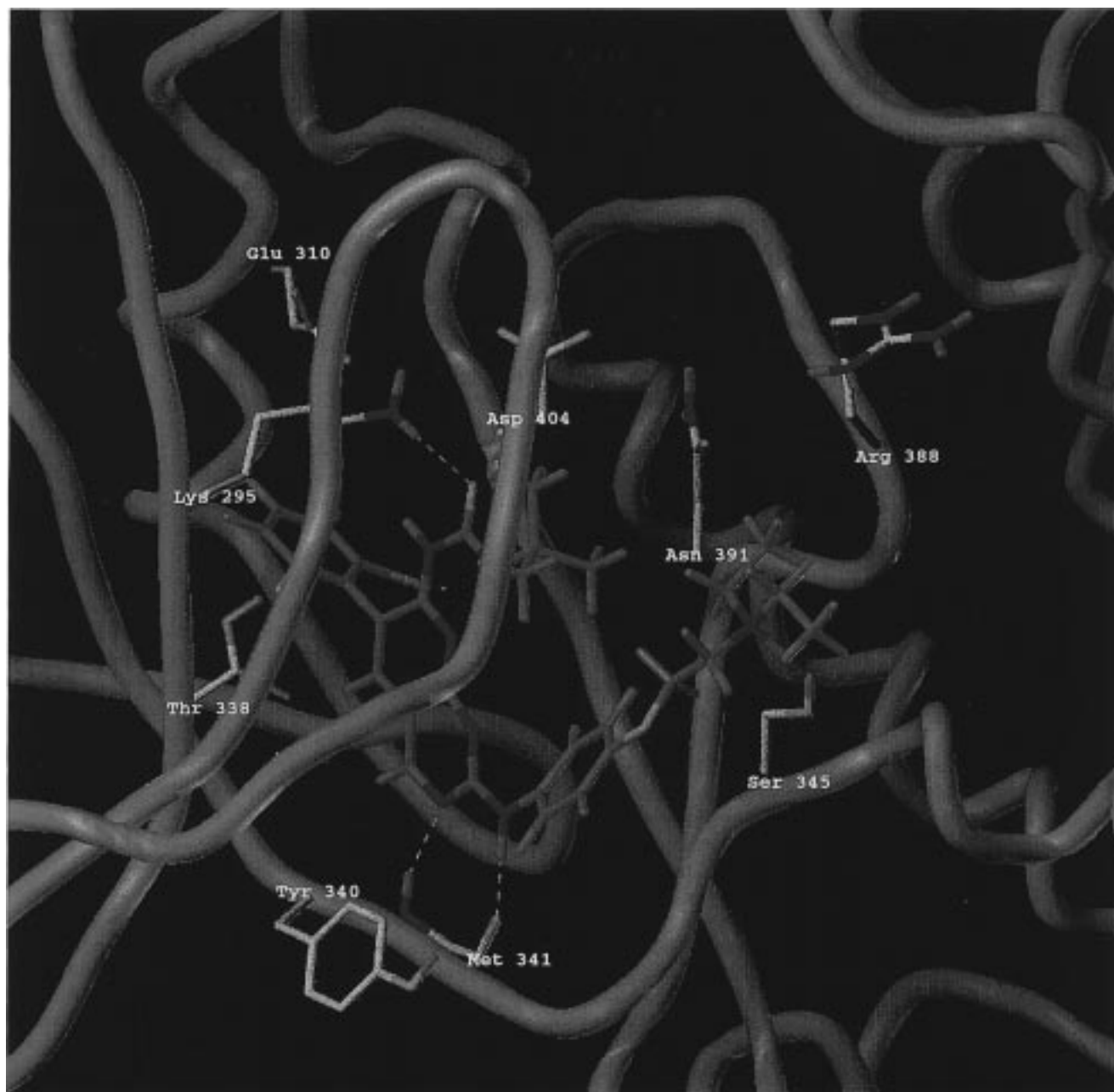
Figure 5. Compound **17** (Table 2) docked into the 3D model of c-Src. For structural series B, the substituted urea appended to the C-7 position is located at the entrance of the pocket near the binding site for the ribose ring of ATP. Larger substituents such as cyclohexyl, benzyl, or phenyl of compounds **14**−**16** extend out of the binding pocket and reach out to residues located in the hinge region.

binding pocket, amino acid differences are present on strands 4, 5, and 8 in tyrosine kinases. These differences change the shape of the pocket and thus might account for the selectivity patterns seen when different substituents are introduced into the 6-phenyl ring. For example, Ile 336 on strand 5 in c-Src and PDGFr is changed to Val 559 in FGFr and Leu 764 in EGFr (Figure 2). Thr 338 on strand 5 of c-Src, EGFr, and PDGFr corresponds to Val 561 in FGFr kinase. Val 323 on strand 4 of c-Src and PDGFr corresponds to Ile 545 in FGFr kinase and Cys 751 in EGFr kinase. Ala 403 on strand 8 of c-Src and FGFr kinases corresponds to Thr 830 in EGFr kinase and Cys 842 in PDGFr kinase. In particular, in the 3D model of FGFr kinase Val 559 on strand 5 is located directly next to one of the 3,5-dimethoxy groups of the 6-phenyl substituent of FGF-

selective inhibitors and thus might be responsible for the selectivity. In PDGFr, EGFr, and c-SRC a larger Ile or Leu is present which might reduce the size of the pocket and thus prevent binding.

Structural differences in this pocket can also explain why cyclin-dependent kinases are insensitive to these inhibitors. Extra bulk is introduced on strand 5 by the larger Phe amino acid residue (Phe 80 in CDK2). For this kinase, a steric clash between the Phe side chain and the 6-phenyl ring of the pyrido[2,3-*d*]pyrimidines is apparent from our modeling studies. Figure 7 shows the primary structure alignment of PKA, tyrosine kinases, CDK2, and CDK4 in the ATP binding site. Residues which are proposed to be responsible for the selectivity are colored in green and indicated with a star.
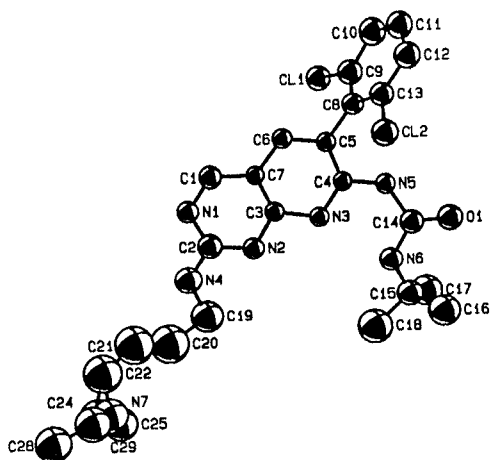
Figure 6. ORTEP diagram showing the X-ray structure of compound **13** (Table 2). The 2,6-dichlorophenyl moiety is rotated out of plane by 67°. The urea substituent at C-7 has a *cis*-amide bond and forms an intracellular hydrogen bond with N-8 of the pyrido[2,3-*d*]pyrimidine ring.

A second important structural factor in conferring selectivity may be specific conformational changes observed in this region for different protein kinases. A comparison of the X-ray structures of the inactive (apo) form of FGFr kinase and c-Src shows large differences in this binding pocket that are due to unique conformational reorientations in the αC helix, strand 8, the activation loop, and the glycine-rich loop.

In summary, both side-chain substitutions and conformational differences across a range of kinases may contribute to the specificity patterns observed for our inhibitors. The SAR data reveal that inhibitors from both structural series A and B generally are less potent toward PDGFr and EGFr kinases relative to FGFr and c-Src. Whether these data point to a true selectivity, due to structural differences within these kinases, or whether different enzyme assay conditions are responsible for this pattern is difficult to determine at this time. Cell-based assays and site-directed mutagenesis are needed to further address this question.

Conclusions

Given the high degree of amino acid conservation within the ATP binding pocket of protein kinases, the design of highly selective ATP-competitive inhibitors was long believed to be impossible. This notion has been refuted by recent publications of several classes of ATP-competitive inhibitors that display high potency and specificity toward a number of isolated serine/threonine and tyrosine kinases. These inhibitors generally are made up of a heterocyclic core that roughly mimics adenine. Like adenine, they form hydrogen bonds with the extended coil stretch of the kinase. Interestingly, however, the most potent and selective inhibitors show a hydrogen-bonding pattern different from that found for ATP. For example, in the highly selective quinazoline EGFr inhibitors, two hydrogen bond acceptors are present. N-1 of the quinazoline ring forms a hydrogen bond with the backbone NH of Met 769, analogous to the hydrogen bond formed by N-1 of adenine. N-3 forms a hydrogen bond with the hydroxyl of Thr 766 located deep in the binding pocket on strand 5. A corresponding hydrogen bond is not formed by the adenine of ATP.[19]

In the highly selective pyridinylimidazole p38 MAP kinase inhibitors, there is a single hydrogen bond formed by the pyridyl ring nitrogen to the main-chain amino group of residue 109, which is analogous to that observed for N-1 of adenine.[20] The pyrido[2,3-*d*]pyrimidine inhibitors discussed herein are proposed to have a hydrogen-bonding pattern identical to that of olomoucine. Moreover, part of these selective inhibitors (the 6-phenyl substituent of the pyrido[2,3-*d*]pyrimidine inhibitors, the 3′-iodophenyl group of the p38 MAP kinase inhibitor, and the *m*-bromoanilino substituent of the EGFr inhibitors) protudes away from the ATP envelope and binds in a deep pocket of moderate size made up of strands 4, 5, and 8 and the αC helix. In particular, the unique amino acid conformation in each protein kinase in this pocket might help to confer specificity and high-affinity binding for these inhibitors.

On the other hand, inhibitors exist, which exert their selectivity by inducing specific conformational changes in the ATP binding pocket. The X-ray structure of FGFr kinase complexed with Su5402 reveals a hydrogen-bonding pattern identical to that of ATP and a third hydrogen bond between the side-chain amide of Asn 568 in the hinge region and the carboxyethyl group of Su5402.[21] In particular, for Su5402, specificity for FGFr kinase seems to be achieved by a specific conformational change in the glycine-rich loop. Upon inhibitor binding this loop closes down, and a highly conserved Phe 489 comes into close contact to interact specifically with the oxindole of Su5402, thus conferring specificity.

Signaling for a large number of cellular functions, including cell growth and differentiation, is modulated by a variety of receptor and nonreceptor protein tyrosine kinases and by their ability to phosphorylate tyrosine residues in specific proteins.[1] Therefore, the selective inhibition of specific kinases represents an attractive approach for the pharmaceutical intervention of a number of disease states. For example, inhibitors of PDGFr kinase have been shown to reduce the proliferative responses of vascular smooth muscle cells and thus may prove efficacious toward the treatment of restenosis following balloon angioplasty.[2] Abnormal signaling via Src family nonreceptor tyrosine kinases has been linked to a number of pathophysiological processes including cancer and immunoinflammatory diseases.[22] We believe that the structural information obtained from our studies, as well as those of other laboratories, will assist in the design of inhibitors with the optimal specificity patterns and pharmaceutical properties required to treat many of these diseases. In particular with this structural information we were able to design highly potent "de novo" inhibitors for a number of different protein kinases.

Experimental Section

Protein Modeling. The 3D models of chicken c-Src, human FGFr, mouse PDGFr-β, and human EGFr kinases were constructed with the homology modeling package segmod implemented in Look.[23] The ternary complex of PKA (PDB entry 1ATP) was used as a template for modeling of the tyrosine kinases for the following reasons.

The inhibitors described in this paper inhibit the active form of the protein tyrosine kinases (see Biological Methods) which requires the enzyme in a closed conformation with a specific structural alignment of the αC helix, the β-sheet, and the phosphate binding loop in the N-terminal ATP/inhibitor bind-
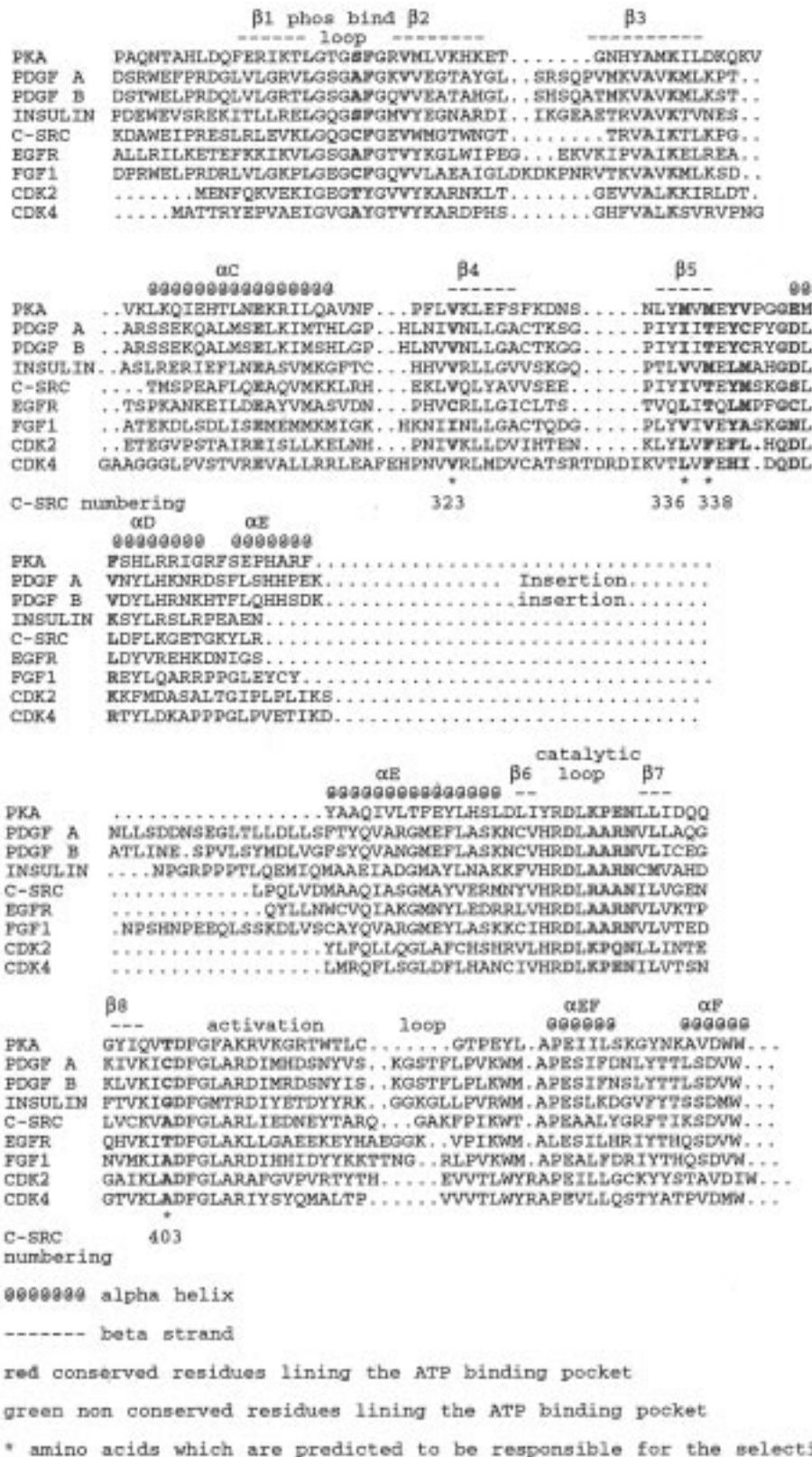
```
                 β1   phos bind β2                    β3
                 ------  loop  ---------          -----------
        PKA      PAQNTAHLDQFERIKTLGTGSFGRVMLVKHKET.......GNHYAMKILDKQKV
        PDGF A   DSRWEFPRDGLVLGRVLGSSGAFGKVVEGTAYGL..SRSQPVMKVAVKMLKPT..
        PDGF B   DSTWELPRDQLVLGRTLGSGAFGQVVEATAHGL..SHSQATHKVAVKMLKST..
        INSULIN  PDEWEVSREKITLLRELGQGSFGMVYEGNARDI..IKGEAETRVAVKTVNES..
        C-SRC    KDAWEIPRESLRLEVKLGQGCFGEVWMGTWNGT.......TRVAIKTLKPG..
        EGFR     ALLRILKETEFKKIKVLGSSGAFGTVYKGLWIPEG...EKVKIPVAIKELREA..
        FGF1     DPRWELPRDRLVLGKPLGSCFGQVVLAEAIGLDKDKPNRVTKVAVKMLKSD..
        CDK2     .......MENFQKVEKIGEGTYGVVYKARNKLT.......GEVVALKKIRLDT.
        CDK4     .....MATTRYEPVAEIGVGAYGTVYKARDPHS.......GHFVALKSVRVPNG

                    αC                   β4                β5
                 999999999999999999    ------           ------    99
        PKA      ..VKLKQIEHTLNEKRILQAVNF...PFLVKLEFSFKDNS.....NLYMVMEYVPGGEM
        PDGF A   ..ARSSEKQALMSELKIMTHLGP..HLNIVNLLGACTKSG.....PIYIITEYCFYGDL
        PDGF B   ..ARSSEKQALMSELKIMSHLGP..HLNVVNLLGACTKGG.....PIYIITEYCRYGDL
        INSULIN  ..ASLRERIEFLNEASVMKGFTC..HHVVRLLGVVSKGQ.....PTLVVMELMAHGDL
        C-SRC    ....TMSPEAFLQEAQVMKKLRH...EKLVQLYAVVSEE......PIYIVTEYMSKGSL
        EGFR     ..TSPKANKEILDEAYVMASVDN..PHVCRLLGICLTS......TVQLITQLMPFGCL
        FGF1     ..ATEKDLSDLISEMEMMKMIGK..HKNIINLLGACTQDG.....PLYVIVEYASKGNL
        CDK2     ..ETEGVPSTAIREISLLKELNH...PNIVKLLDVIHTEN.....KLYLVFEFL.HQDL
        CDK4     GAAGGGLPVSTVREVALLRRLEAFEHPNVVRLMDVCATSRTDRDIKVTLVFEHI.DQDL

                                            *                  *  *
        C-SRC numbering                    323                336 338
                    αD       αE
                 99999999  9999999
        PKA      FSHLRRIGRFSEPHARF.................................
        PDGF A   VNYLHKNRDSFLSHHPEK............Insertion.......
        PDGF B   VDYLHRNKHTFLQHHSDK.................insertion.......
        INSULIN  KSYLRSLRPEAEN.................................
        C-SRC    LDFLKGETGKYLR.................................
        EGFR     LDYVREHKDNIGS.................................
        FGF1     REYLQARRPPGLEYCY.................................
        CDK2     KKFMDASALTGIPLPLIKS.................................
        CDK4     RTYLDKAPPPGLPVETIKD.................................

                                             catalytic
                          αE          β6    loop   β7
                 99999999999999999  --         ---
        PKA      .................YAAQIVLTPEYLHSLDLIYRDLKPENLLIDQQ
        PDGF A   NLLSDDNSEGLTLLDLLSFTYQVARGMEFLASKNCVHRDLAARNVLLAQG
        PDGF B   ATLINE.SPVLSYMDLVGFSYQVANGMEFLASKNCVHRDLAARNVLICEG
        INSULIN  ....NPGRPPPTLQEMIQMAAEIADGMAYLNAKKFVHRDLAARNCMVAHD
        C-SRC    ...........LPQLVDMAAQIASGMAYVERMNYVHRDLRAANILVGEN
        EGFR     ...........QYLLNWCVQIAKGMNYLEDRRLVHRDLAARNVLVKTP
        FGF1     .NPSHNPEEQLSSKDLVSCAYQVARGMEYLASKKCIHRDLAARNVLVTED
        CDK2     ...............YLFQLLQGLAFCHSHRVLHRDLKPQNLLINTE
        CDK4     ...............LMRQFLSGLDFLHANCIVHRDLKPENILVTSN

                 β8                                   αEF        αF
                 ---      activation      loop     999999     999999
        PKA      GYIQVTDPGFAKRVKGRTWTLC.......GTPEYL.APEIILSKGYNKAVDWW...
        PDGF A   KIVKICDFGLARDIMHDSNYVS..KGSTFLPVKWM.APESIFDNLYTTLSDVW...
        PDGF B   KLVKICDFGLARDIMRDSNYIS..KGSTFLPLKWM.APESIFNSLYTTLSDVW...
        INSULIN  FTVKIGDFGMTRDIYETDYYRK..GGKGLLPVRWM.APESLKDGVFYTSSDMW...
        C-SRC    LVCKVADFGLARLIEDNEYTARQ...GAKFPIKWT.APEAALYGRFTIKSDVW...
        EGFR     QHVKITDFGLAKLLGAEEKEYHAEGGK..VPIKWM.ALESILHRIYTHQSDVW...
        FGF1     NVMKIADFGLARDIHHIDYYKKTTNG..RLPVKWM.APEALFDRIYTHQSDVW...
        CDK2     GAIKLADFGLARAFGVPVRTYTH.....EVVTLWYRAPEILLGCKYYSTAVDIW...
        CDK4     GTVKLADFGLARIYSYQMALTP......VVVTLWYRAPEVLLQSTYATPVDMW...

                       *
        C-SRC          403
        numbering

        9999999 alpha helix

        ------- beta strand

        red conserved residues lining the ATP binding pocket

        green non conserved residues lining the ATP binding pocket

        *  amino acids which are predicted to be responsible for the selectivity of the inhibitors
```

Figure 7. Sequence alignment of the protein kinase template PKA with PDGFr-α, PDGFr-β, insulin receptor, c-Src, EGFr, FGF1, CDK2, and CDK4 kinases in the ATP binding region. Conserved residues lining the ATP binding pocket are shown in red. Nonconserved residues lining the ATP binding pocket are shown in green. Residues which line the 6-phenyl substituent binding pocket and which are predicted to be responsible for the selectivity are indicated with green stars.

ing pocket. This conformation is present in the high-resolution X-ray structure of the ternary complex of PKA.[10]

X-ray structures of the catalytic domain of the FGF (PDB entry 1FGK), c-Src (PDB entry 1FMK), and Hck (PDB entry 1ADE5) have been published recently but could not be used in these modeling studies because the structures were crystallized in the inactive conformation which is structurally different from the active conformation of protein kinases.[16–18] For example, in the inactive form of Hck and c-Src, the αC helix, which is an essential part of the inhibitor binding pocket, is

swung out of the active site and faces into solvent. Therefore the conformation in the deep pocket where the 6-phenyl ring of the pyrido[2,3-*d*]pyrimidine inhibitor binds is different. Furthermore catalytically important residues are not lined up: for example, a salt bridge between Glu 310 and Lys 295 in Hck or the corresponding residues in c-Src is not present (the corresponding Lys 72 and Glu 91 form a salt bridge in PKA). In the X-ray structure of the inactive form of the FGFr tyrosine kinase, the ATP binding site is in a more open conformation and in addition large parts of the structure are missing due to insufficient electron density (e.g., the phosphate binding loop, the activation loop, a large insertion after the extended coil stretch).[18]

Shortly after completion of this study, the structure of the active but unligated form of Lck (PDB entry 3LCK) became available[24] and the X-ray structure of the activated form of the insulin receptor tyrosine kinase (IRK3P) was published[25] (PDB entry 1IR3). Both enzymes belong to the tyrosine kinase family and are close homologues of the FGFr, EGFr, PDGFr, and c-Src tyrosine kinase family.

As predicted, the conformation in the ATP binding site of these activated kinases is almost identical to that of active PKA, and ultimately, the catalytically important residues Lys 273 in Lck (Lys 72 in PKA and Lys 1030 in IRK3P), Glu 288 (Glu 91 in PKA and Glu 1047 in IRK3P), Asp 382 (Asp 184 in PKA and Asp 1150 in IRK3P), Asp 364 (Asp 162 in PKA and Asp 1132 in IRK3P), and Asn 369 (Asn 169 in PKA and Asn 1137 in IRK3P) are all in equivalent positions in Lck, PKA, and IRK3P. A structural superimposition of the Cα atoms between PKA and Lck reveals rms deviations of only 1.18 Å in the N-terminal domain and 1.2 Å in the C-terminal domain despite the low primary sequence identity of 19%. The only structural difference occurs in the glycine-rich loop, which is in an open conformation in Lck because the enzyme was crystallized without ATP and peptide (this loop normally closes down upon ATP and substrate binding).[18] A detailed decription of the structural comparison of Lck and PKA is given in ref 24.

Finally, analogous interactions for the adenine and the ribose are observed in IRK3P compared to the ternary PKA structure, except that O3′ is hydrogen-bonded to Arg 1136 (in PKA O3′ binds directly to the carbonyl oxygen of Glu 170).

These structural homologies in the ATP binding site fully justify the use of PKA as a template for the model construction of EGFr, PDGFr, FGFr, and c-Src kinases. The inactive comformation of Hck, c-Src, or FGFr would not represent better templates because of the different relative orientation of secondary structures in the ATP binding site.

Basis for the protein modeling was the alignment of the template PKA with the target proteins EGFr, FGFr, PDGFr, and c-Src (as shown in Figure 7). The overall amino acid identity compared to PKA is with 18−35% rather low but goes up to 60−80% amino acid identity in the ATP binding site. Extensive primary structure alignments have been published by Hanks et al. by aligning more than 400 different protein kinases.[12] This has led to very precise identification of conserved primary and secondary structure elements in the protein kinase family. Basis for our alignment was therefore the alignment published by Hanks and the structural alignment of tyrosine kinases and PKA as published by Hubbard et al.[25]

Segmod[26] implemented in Look[23] was used to build the protein models based on the alignment. In the first step segmod divides the sequence to be modeled into short segments. A database of highly refined X-ray structures is then searched for matching segments, which are fitted onto the framework of the template structure. Three criteria are used to chose a matching database segment: amino acid sequence similarity with the target structure, conformational similarity with the template structure, and compatibility with the target structure. Ten independent models are built based on different random choices and then averaged. Finally, the protein model undergoes energy minimization with the force-field program Encad[26] to optimize the geometry and nonbonded interactions.

The resulting models of PDGFr, FGFr, c-Src, and EGFr were analyzed with Protable implemented in Sybyl 6.2[27] to check backbone conformation, stereochemistry, solvent-accessible surface areas, and side-chain conformational probabilities. The tyrosine kinase models were superimposed onto the X-ray structure of the template PKA with the program InsightII.[28] Rms deviations in the aligned regions (excludes insertions and deletions in loop areas) for the Cα atoms were 0.94 Å for EGFr, 1.27 Å for PDGFr, 1.06 Å for FGFr, and 1.11 Å for c-Src. In addition, superimposition of the Cα atoms of the N-terminal ATP/inhibitor binding domain of the tyrosine kinase models with the N-terminal domain of Lck gave rms values of 1.15 Å for EGFr, 1.25 Å for PDGFr, 1.19 Å for FGFr, and 1.13 Å for c-Src kinase (the phosphate binding loop was excluded from the superimposition because of the open conformation in Lck).

Additionally, the N- and C-terminal domains of the FGFr and c-Src models were independently superimposed onto their published X-ray structures of the inactive form of the FGFr and c-Src kinases to check the primary and secondary structure alignment. The primary structure alignment of both modeled kinases to their experimental structures was entirely correct in the N- and C-terminal domains as well as their secondary structure alignments with the exception of the last C-terminal αI helix, due to missing primary structure homology and structural differences between PKA, Hck, c-Src, FGFr, and Lck. For the same reason, the conformation of the random coil area in the C-terminal domain of both FGFr and c-Src kinases between αH and αI showed structural deviation from the experimental structures. This is not surprising, since without any primary structure homology random coil areas are generally modeled incorrectly by any protein-modeling program. In addition, in the c-Src model, the kinase insert region between αD and αE showed structural deviation from the experimental structure. The α-helices αE, αF, αG, and αH in the C-terminal domain superimposed with an rms of 1.45 Å between the c-Src model and the experimental structure and 1.58 Å between the FGF model and the experimental FGF structure.

In conclusion, these analyses indicate that the structural compatibility between the models and the experimental structures PKA and Lck in the N-terminal ATP/inhibitor binding domain and in most parts of the C-terminal domain is very good. This fully justifies the use of PKA as a template for the model building of the tyrosine kinases.

Small Molecule Modeling. The basic structure of the 7-urea-substituted pyrido[2,3-*d*]pyrimidines (structural class B, Table 2) was derived from small molecule X-ray crystallographic data. In the X-ray structure, the urea substituent has a *cis*-amide conformation and forms an internal hydrogen bond with N-8 of the pyrido[2,3-*d*]pyrimidine template (Figure 5). The phenyl ring substituent at C-6 is rotated out of plane by 67°, due to the presence of the 2,6-dichloro substituents. In the X-ray structure, the 2-NH(CH₂)₃-N-Me-piperazine side-chain substituent adopts an extended conformation; in solution this side chain might adopt different conformations due to its flexibility.

Inhibitors from structural class A (Table 1) were constructed in Sybyl 6.2 using the X-ray structure of structural class B as template. Different amino substituents were added at C-2 using the fragment database in Sybyl 6.2.[27] The inhibitors were geometry-optimized with the MM3 force field[29] implemented in Sybyl 6.2. For compounds with an aniline substituent at the C-2 position, a conformational search was performed with MM3 with two rotatable bonds defined between the pyrido[2,3-*d*]pyrimidine template and the aniline ring. Two minimum-energy conformations were found. In both conformations, the aniline ring is coplanar with the pyrido[2,3-*d*]pyrimidine ring system. The conformation with the aniline ring vicinal to the N-3 of the pyrido[2,3-*d*]pyrimidine is slightly more energetically favorable (6.99 kcal/mol) compared to the conformation with the aniline ring vicinal to N-1 (7.05 kcal/mol). A 30° out-of-plane rotation of the phenyl ring increases slightly the internal energy to 12.9 and 12.7 kcal/mol, respectively.

Charges for small molecule inhibitors were derived from the semiempirical molecular orbital package Mopac using the MNDO approach.[30] Inhibitors were docked manually into the ATP binding site and geometry-optimized with the Tripos force field implemented in Sybyl 6.2 to optimize hydrogen-bonding interactions and to relieve unfavorable steric contacts.

X-ray Structure Determination. Compound **13** ($C_{26}H_{35}N_6$-OCl_2, molecular weight = 518.51) was crystallized as yellow needles from ethanol solutions. X-ray data were collected on an Enraf-Nonius CAD-4 diffractometer using CuK radiation ($\lambda = 1.541\,84$ Å). The cell constants and an orientation matrix for data collection were determined from the centered angles of 25 reflections. X-ray diffraction data were collected to a maximum 2θ of 114.5°. A total of 4307 reflections were collected, of which 3914 were unique and not systematically absent. Lorentz and polarization corrections were applied as well as the data as well as an empirical absorption correction based on a series of ψ scans. The crystal structure was determined by direct methods using SIR-92. A total of 319 reflections with $E > 1.79$ were used to produce a phase set with an absolute figure of merit of 1.09. All 36 heavy atoms in the structure were located from the E map calculated using this phase set. Hydrogen atom positions were located in subsequent difference Fourier maps and added to the structure, but their positions were not refined. The heavy atom parameters including anisotropic temperature factors were refined by full-matrix least-squares using 1345 reflections with intensity greater than 3 times their standard deviation. The final unweighted R-factor is 0.142. The final difference Fourier map was essentially featureless. The highest peak in this map had a height of only 0.54 e/Å.

Biological Methods. 1. PDGFr and FGFr Tyrosine Kinase Enzyme Inhibition Assays.[31,32] Recombinant DNA fragments coding for the tyrosine kinase domains of mouse PDGF-β and human FGF1 were used to overexpress the proteins in baculovirus-infected insect cells. The assay was performed in 96-well plates using cell lysates. The kinase activity of the enzyme lysate was assayed by measuring the incorporation of ^{32}P-labeled phosphate from ATP into trichloroacetic acid-precipitable random copolymer of glutamate/tyrosine (4:1 ratio) in vitro.

2. c-Src Tyrosine Kinase Enzyme Inhibition Assay. The assay is identical to that reported for v-Src except for the source of enzyme (c-Src vs v-Src) and the ATP concentration (40 μM for c-Src vs 4 μM for v-Src).[31] The assay utilized recombinant avian c-Src protein produced in baculovirus-infected insect cells that was immunopurified via a Src-specific monoclonal antibody covalently linked to polystyrene beads. The kinase activity of the enzyme-bead suspension was assayed by measuring the incorporation of ^{32}P-labeled phosphate from ATP into trichloroacetic acid-precipitable random copolymer of glutamate/tyrosine (4:1 ratio) in vitro.

Compound Synthesis. The compounds were synthesized as decribed in PCT Int. Appl. WO 9615128 A2 (1996) and WO 9634867 (1997) as well as in refs 6–8.

Supporting Information Available: Data from the X-ray structure determination of **6** (PD161570) (10 pages). Ordering information can be found on any current masthead page.

References

(1) Saltiel, A. R. Signal transduction pathways as drug targets. *Sci. Am. Sci. Med.* **1996**, *2*, 58–67.
(2) Majesky, M.; Reidy, M.; Bowen-Pope, D.; Hart, C.; Wilcox, J.; Schwartz, S. PDGF ligand and receptor gene expression during repair of arterial injury. *J. Cell. Biol.* **1990**, *111*, 2149–2158.
(3) Jackson, C. L.; Schwartz, S. M. Pharmacology of smooth muscle cell replication. *Hypertension* (*Dallas*) **1992**, *20*, 713–736.
(4) Bornfeld, K. E. Intracellular signaling in arterial smooth muscle migration versus proliferation. *Trends Cardiovasc. Med.* **1996**, *6*, 143–151.
(5) Kelloff, G. J.; Fay, J. R.; Steele, V. E.; Lubet, R. A.; Boone, C. W.; Crowell, J. A.; Sigman, C. C. Epidermal growth factor receptor tyrosine kinase inhibitors as potential cancer chemopreventives. *Cancer Epidemiol. Biomarkers Prev.* **1996**, *5*, 657–666.
(6) Hamby, J. M.; Connolly, C. J.; Schroeder, M. C.; Winters, R. T.; Showalter, H. D. H.; Panek, R. L.; Major, T. C.; Olsewsky, B.; Ryan, M. J.; Dahring, T.; Lu, G. H.; Keiser, J.; Amar, A. A.; Shen, C.; Kraker, A. J.; Slintak, V.; Nelson, J. M.; Fry, D. W.; Bradford, L.; Hallak, H.; Doherty, A. Structure–activity relationships for a novel series of pyrido[2,3-*d*]pyrimidine tyrosine kinase inhibitors. *J. Med. Chem.* **1997**, *40*, 2296–2303.
(7) Klutchko, S. R.; Hamby, J. M.; Boschelli, D. H.; Wu, Z.; Kraker, A. J.; Amar, A. M.; Hartl, B. G.; Shen, C.; Klohs, W. D.; Steinkampf, R. W.; Driscoll, D. W.; Nelson, J. M.; Roberts, B. J.; Stoner, C. L.; Vincent, P. W.; Dykes, D. J.; Panek, R. L.; Lu, G. H.; Major, T. C.; Dahring, T. K.; Hallak, H.; Bradford, L. A.; Showalter, H. D. H.; Doherty, A. M. 2-Substituted aminopyrido[2,3-*d*]pyrimidin-7(8H)-ones. Structure–activity relationships against selected tyrosine kinases and in vitro and in vivo anticancer activity. Manuscript in preparation.
(8) Connolly, C. J. C.; Hamby, J. M.; Schroeder, M. C.; Barvian, M.; Lu, G. H.; Panek, R. L.; Amar, A.; Shen, C.; Kraker, A. J.; Fry, D. W.; Klohs, W. D.; Doherty, A. Discovery and structure-activity studies of a novel series of pyrido[2,3-*d*]pyrimidine tyrosine kinase inhibitors. *Bioorg. Med. Chem. Lett.* 7, 2415–2420.
(9) (a) Schroeder, M. C.; Hamby, J. M.; Grohar, P. J.; Winter, R. T.; Connolly, C. J. C.; Showalter, H. D. H.; Kraker, A. J.; Amar, A. M.; Shen, C.; Lu, G. H.; Dahring, T. K.; Panek, R. L.; Major, T. C.; Doherty, A. M. The synthesis and SAR of pyrido[2,3-*d*]-pyrimidine-2,7-diamines in the development of potent water soluble tyrosine kinase inhibitors. Presented at the National Medicinal Chemistry Symposium, Ann Arbor, MI, June 1996; Abstract No. 4. (b) Blankley, C. J.; Doherty, A. M.; Hamby, J. M.; Panek, R. L.; Schroeder, M. C.; Showalter, H. D. H.; Connolly, C. J. Preparation of 6-aryl pyrido[2,3-*d*]pyrimidines and naphthyridines for inhibiting protein tyrosine kinase-mediated cellular proliferation. PCT Int. Appl. WO 9615128 A2, 1996.
(10) Zheng, J.; Trafny, E. A.; Knighton, D. R.; Xuong, N.-H.; Taylor, S. S.; Ten Eyck, L. F.; Sowadsky, J. M. 2.2 A refined crystal structure of the catalytic subunit of cAMP-dependent protein kinase complexed with MnATP and a peptide inhibitor. *Acta Crystallogr.* **1993**, *D49*, 362–365.
(11) Schulze-Gahmen, U.; Brandsen, J.; Jones, H. D.; Morgan, D. O.; Meijer, L.; Vesely, J.; Kim, S.-H. Multiple modes of ligand recognition: Crystal structures of cyclin-dependent protein kinase 2 in complex with ATP and two inhibitors, olomoucine and isopentyladenine. *Proteins: Struct. Funct. Genet.* **1995**, *22*, 378–391.
(12) Hanks, S. K.; Quinn, A. M. Protein kinase catalytic domain sequence database: Identification of conserved features of primary structure and classification of family members. *Methods Enzymol.* **1991**, *200*, 38–62.
(13) De Bondt, H. L.; Rosenblatt, J.; Jancarik, J.; Jones, H. D.; Morgan, D. O.; Kim, S. H. Crystal structure of cyclin-dependent kinase 2. *Nature* **1995**, *363*, 595–602.
(14) Owen, D. J.; Noble, M. E. M.; Garman, E. F.; Papageorgiou, A. C.; Johnson, L. N. Two structures of the catalytic domain of phosphorylase kinase: an active protein kinase complexed with substrate analogue and product. *Structure* **1995**, *3*, 467–482.
(15) Zang, F.; Strand, A.; Robbins, D.; Cobb, M. H.; Goldsmith, E. J. Atomic structure of the MAP kinase ERK2 at 2.3 A resolution. *Nature* **1994**, *367*, 704–711.
(16) Xu, W.; Harrison, S. C.; Eck, M. J. Three-dimensional structure of the tyrosine kinase c-Src. *Nature* **1997**, *385*, 595–602.
(17) Sicheri, F.; Moarefi, I.; Kuriyan, J. Cystal structure of the Src family tyrosine kinase Hck. *Nature* **1997**, *385*, 602–609.
(18) Mohamadi, M.; Schlessinger, J.; Hubbard, S. Structure of the FGF receptor tyrosine kinase domain reveals a novel autoinhibitory mechanism. *Cell* **1996**, *86*, 577–587.
(19) Wilson, K. P.; McCaffrey, P. G.; Hsiao, K.; Pazhanisamy, S.; Galullo, V.; Bemis, G. W.; Fitsgibbon, M. J.; Caron, P. R.; Murcko, M. A.; Su, M. S. S. The structural basis for the specificity of pyridinylimidazole inhibitors of p38 MAP kinase. *Chem. Biol.* **1997**, *4*, 423–431.
(20) Palmer, B. D.; Trumpp-Kallmeyer, S.; Fry, D. W.; Nelson, J. M.; Showalter, H. D. H.; Denny, W. A. Tyrosine kinase inhibitors. 11. Soluble analogues of pyrrolo- and pyrazoloquinazolines as epidermal growth factor receptor inhibitors: synthesis, biological evaluation, and modeling of the mode of binding. *J. Med. Chem.* **1997**, *40*, 1519–1529.
(21) Mohamadi, M.; McMahon, G.; Sun, L. T.; Tang, C.; Hirth, P.; Yeh, B. K.; Hubbard, S. R.; Schlessinger, J. Structures of the tyrosine kinase domain of fibroblast growth factor receptor in complex with inhibitors. *Science* **1997**, *276*, 955–960.
(22) Bolen, J. B.; Penhallow, R. C.; Burkhard, A. L. Signal transduction by the src family of tyrosine protein kinase. In *Encyclopedia of Cancer*; Bertino, J., Ed.; Academic Press: San Diego, CA, 1997; pp 1657–1668.
(23) Look; Molecular Applications Group, 445 Sherman Ave, Suite T, Palo Alto, CA 94306.

(24) Yamaguchi, H.; Hendrickson, W. A. Structural basis for activation of human lymphocyte kinase Lck upon tyrosine phosphorylation. *Nature* **1996**, *384*, 484−489.

(25) Hubbard, S. Crystal structure of the activated insulin receptor tyrosine kinase in complex with peptide substrate and ATP analogue. *EMBO* **1997**, *16*, 5572−5581.

(26) Levitt, M. Accurate modeling of protein conformation by automatic segment matching. *J. Mol. Biol.* **1992**, *226*, 507−533.

(27) Sybyl, molecular modeling software; Tripos E & S, 6548 Clayton Rd, St. Louis, MO 62117.

(28) InsightII/Discover; Biosym/MSI, 9685 Scranton Rd, San Diego, CA 92121-2777.

(29) Allinger, N. L.; Yuh, Y. H.; Lii, J. H. Molecular mechanics. The MM3 force field for hydrocarbonns. 1. *J. Am. Chem. Soc.* **1989**, *111*, 8551−9566.

(30) Dewar, M. J. S.; Thiel, W. Ground states of molecules. The MNDO method, approximations and parameters. *J. Am. Chem. Soc.* **1977**, *99*, 4899.

(31) Panek, R. L.; Lu, G. H.; Klutchko, S. R.; Batley, B. L.; Dahring, T. K.; Hamby, J. M.; Hallak, H.; Doherty, A. M.; Keiser, J. A. In vitro pharmacological characterization of PD166285, a new broadly active protein tyrosine kinase inhibitor. *J. Pharmacol. Exp. Ther.* **1997**, *283*, 1433−1444.

(32) Dahring, T. K.; Lu, G. H.; Hamby, J. M.; Batley, B. L.; Kraker, J.; Panek, R. L. Inhibition of growth factor-mediated tyrosine phosphorylation in vascular smooth muscle by PD 089828, a new synthetic protein tyrosine kinase inhibitor. *J. Pharmacol. Exp. Ther.* **1997**, *281*, 1446−1456.